

**Tensile strength of rubber described via the formation and rupture of load-bearing polymer chains**Reinhard Hentschke *School of Mathematics and Natural Sciences Bergische Universität, D-42097 Wuppertal, Germany*

(Received 30 January 2022; accepted 14 July 2022; published 29 July 2022)

A theoretical picture describing the tensile strength  $\sigma_T$  of elastomers is developed.  $\sigma_T$  is composed of three factors: (1) the tensile strength of individual polymer load-bearing chains (LBCs) according to Eyring's theory, (2) an occupation number of LBC states using Fermi statistics, and (3) an excluded volume factor reducing the number of possible LBCs due to the presence of filler particles or crosslinks between polymers. This description is compared to experimental tensile strengths of carbon black (N339)-filled EPDM (Keltan 4450) as well as to other experiments in the literature studying the effects of temperature, filler concentration, and particle size as well as crosslink density.

DOI: [10.1103/PhysRevE.106.014505](https://doi.org/10.1103/PhysRevE.106.014505)**I. INTRODUCTION**

Filled rubbers are exceedingly complex materials whose chemo-physical behavior results from a multitude of mechanisms spanning wide ranges on the spatial and temporal scales. Construction of quantitative theories describing this behavior or predicting useful novel properties in response to changes in composition is nearly impossible. Faced with this predicament the goal should be the development of qualitative theories, including as many of the relevant variables as possible, in order to understand and utilize the interdependencies between variables and their effect on rubber properties. Here we focus on such a theory for tensile strength of filled rubber.

The tensile strength of rubber composites began to be a focus of theoretical work in “soft matter physics” in the 1940s and by the 1950s and early 1960s a number of theories had been developed [1–3]. Bueche's work certainly is the most detailed on the subject during this period. The key elements of his theories are highly strained polymer chains and the hierarchical load transfer to secondary chains when the primary chains rupture. Subsequently, however, it seems, systematic theoretical work subsided and was replaced by more qualitative discussions (see, for instance, Dannenberg's excellent review [4]), and no unifying theoretical picture has emerged thus far [5]. This is in stark contrast to the many developments on the experimental side [5]. New product requirements, like the prevention or reduction of microplastics, which were not foreseen in the aforementioned decades are current technological challenges [6]. But whatever the intended purpose of a new rubber material may be, tensile strength is always among the standard measurements forming the basis for its evaluation [7,8].

Measuring the tensile strength  $\sigma_T$  vs (active) filler volume fraction  $\phi$  reveals an s-shaped curve, i.e., a slow initial increase followed by a significantly steeper increase, which levels off into a plateau or rather a broad maximum due to the decrease of the tensile strength at high volume fractions. The clarity of this observation depends on the number of data points and their  $\phi$  range. Until recently there were numerous yet, each by itself, not entirely convincing measurements

supporting this general picture [9–14]. The s-shape of  $\sigma_T$  vs  $\phi$  was demonstrated conclusively by Plagge [15] for carbon black (CB) filled ethylene-propylene-diene rubber (EPDM) vulcanizates. Plagge shows that the observed inflection point is a function of temperature. Additionally, his data collapse onto a master curve if represented in the form  $\sigma_T/\sigma_{T,o}(T)$  vs  $\phi/\phi_c(T)$ , where both  $\sigma_{T,o}(T)$  and  $\phi_c(T)$  are functions of temperature  $T$ . In his paper Plagge also suggest a theoretical model, which is based on a combination of two effects. One is the rupture of single polymer chains described by an Eyring-like rate expression. The second is the “meandering” and the “scattering” of a propagating crack by the filler particles inside the composite. Both contributions in Plagge's theory depend on temperature through the introduction of a Williams-Landel-Ferry shift factor. This theory, however, applies only to filled elastomers.

The s shape of  $\sigma_T$  vs  $\phi$  is suggestive of an underlying percolation phenomenon. This idea is pursued by Wang *et al.* [13], who interpret their results of an extensive study of nanostrengthening via nanoparticle addition to styrene-butadiene rubber (SBR) and EPDM along this line. Percolation of nanoparticles inside, for instance, an elastomer matrix is well known. During the initial mixing the filler is dispersed within the polymer matrix. Subsequent filler flocculation then leads to the formation of agglomerates [16]. Beyond a certain filler volume fraction,  $\phi_p$ , the agglomerates begin to form percolating networks traversing the matrix [5,16,17].  $\phi_p$  is established via conductivity measurements using conducting fillers like CB [18]. The percolation threshold  $\phi_p$  thus established correlates quite well with a marked increase of the storage modulus  $\mu'(u, \phi)$  in the limit of small strain amplitude  $u$ . More precisely, for small  $\phi$  below  $\phi_p$  the storage modulus usually is well described by  $\mu'(u, \phi) = \mu'(u, 0)(1 + 2.5\phi + c_1\phi^2)$ , where  $c_1$  is a constant coefficient [17]. Above  $\phi_p$  the  $\phi$  dependence of the storage modulus is best described by a power law,  $\mu'(u, \phi) \sim (\phi/\phi_p)^y$ , where  $y \approx 3.5$  (see Sec. 10.2 in Ref. [19]) or close to this value [20]. If in this filler regime  $\mu'(u, \phi)$  is measured as function of  $u$ , a pronounced decrease of  $\mu'(u, \phi)$  is found (Payne effect [19]). Typically, this decrease, which commonly is explained by the “breakdown”

of the filler network, occurs between 1% and 10% strain. This strain range, however, is significantly below the strain regime at which tensile failure of the sample is observed. Nevertheless, it not unreasonable to assume that the gaps now formed between separated particles or particular aggregates are “bridged” by stretched polymer chains carrying the load and physically attached to either particle surface (an idea already discussed by Dannenberg [4]), i.e., a “mechanical percolation” replaces the “electrical percolation.” It is this idea which is underlying the interpretation of the measurements in Ref. [13]. However, as observed by Plagge and by Wang *et al.*,  $\phi_c(T)$  depends on temperature, while  $\phi_p$  does not. This does not mean that Wang *et al.* are wrong, but it means that  $\phi_c(T)$  and  $\phi_p$  are not simply the same.

It is important to emphasize that tensile strength is only one aspect of the “reinforcement of polymer nanocomposites” in general or “reinforcement of elastomers” in particular. However, even reinforcement of elastomers by itself is a wide field and this is not the place for a comprehensive overview (good sources are Refs. [5,19,21]). Much of the theoretical research on rubber reinforcement has focused on the effects which fillers and compatibilizing agents, including other rubber components, have on the dynamic moduli in the low and medium strain range including the Payne effect (with the notable exception of strain induced crystallization [22] usually observed at considerable strain). In this regime reinforcement is largely due to the filler agglomerates and, at higher filler concentration, the agglomerate network embedded in rather strongly bound polymer layers. In the present model of tensile strength, the original agglomerate network no longer exists due to the large strains involved. The concept of the “polymer layer” is replaced by an approach that focusses on the individual polymer chain, which nevertheless must be able to attach itself to the filler surface, mainly via physisorption, in order to bear load.

In this work we discuss an explanation for the observed shape of  $\sigma_T$  vs  $\phi$  which is different from the percolation idea suggested by Wang *et al.* Nevertheless, the main elements still are load-bearing chains (LBCs) between particles or particles and crosslinks or between crosslinks. Here their probability of occurrence is described by Fermi statistics, which explains the temperature dependence of  $\phi_c(T)$ . In a basic representation  $\sigma_T$  is composed of three factors: (1) the tensile strength of individual polymer LBCs according to Eyring’s theory, (2) an occupation number of LBC states using Fermi statistics, and (3) an excluded volume factor reducing the number of possible LBC due to the presence of filler particles or crosslinks between polymers. This description is compared to experimental tensile strengths of CB (N339)-filled EPDM (Keltan 4450) as well as to other experiments in the literature studying the effects of temperature, filler concentration, and particle size as well as crosslink density.

## II. THEORY OF ELASTOMER TENSILE STRENGTH IN TERMS OF FORMATION AND RUPTURE OF LOAD-BEARING POLYMER CHAINS

In the following  $\sigma_T$  is the tensile strength of an elastomer composite, which here is expressed as a product of three

factors,

$$\sigma_T = \sigma_{T,o} \langle n \rangle (1 - \phi). \quad (1)$$

The quantity  $\sigma_{T,o}$  denotes the tensile strength of an individual polymer LBC,  $\langle n \rangle$  is an occupation number of a “load-bearing state,” and  $(1 - \phi)$ , where  $\phi$  is the filler volume fraction, is an excluded volume factor.

$\sigma_{T,o}$  may be described in terms of the Eyring expression for the chain rupture rate  $k_r$ , which is

$$k_r = \nu A \exp[-(E_b - f d)/RT]. \quad (2)$$

The quantity  $\nu$  is a molecular attempt frequency and  $A$  is a factor essentially composed of the partition functions on the two sides of the reaction equation.  $E_b$  is an activation energy along the path of chain rupture. The chain, due to the externally applied macroscopic stress, experiences a tensile force  $f$ , which acts along the activation length  $d$ . In the following  $f d$  is replaced by  $q \sigma_{T,o} \nu$ , where  $\nu = a d$ .  $a$  is the cross section of a chain and  $q (> 1)$  is a factor, accounting for the expectation that the stress on an individual LBC exceeds the overall macroscopic tensile stress on the sample. Here it is assumed that  $\sigma_{T,o}$  is proportional to the inverse rupture rate,

$$\sigma_{T,o} \propto \frac{1}{k_r}. \quad (3)$$

This stipulation, asserting the existence of a critical chain rupture rate, is analogous to a similar one already employed by Büche [23]. We shall return to this point in the discussion. Relation (3) yields

$$\ln s = \frac{e - q s}{t} - c. \quad (4)$$

Here  $s$ ,  $e$ , and  $t$  are reduced quantities defined via  $s = \sigma_{T,o} \nu / (RT_o)$ ,  $e = E_b / (RT_o)$ , and  $t = T / T_o$ .  $T_o$  is a convenient reference temperature (in the following  $T_o = 273.15$  K).  $c$  is a constant which has absorbed the other constants in Eqs. (2) and (3). Note that  $A = A(T)$ , i.e.,  $A$  does depend on temperature. But the attendant temperature variation [ $O(\ln T)$ ] in Eq. (4) is weak compared to the  $1/T$  dependence and will be neglected here. Equation (4) is an implicit equation for  $\sigma_{T,o}$  and is solved numerically. In principle the quantities  $e$ ,  $q$ ,  $\nu$ , and  $c$  are adjustable parameters. Even though  $q$  and  $\nu$  are not independent, i.e.,  $q \nu$  is the adjustable parameter, it is advantageous to keep them separate. Note that  $\nu$ , defined above, possesses a distinct physical meaning and can be estimated separately. This makes it easier to find and interpret reasonable values of  $q$ . Here we use  $\nu = (0.5 \text{ nm})^3 \approx 0.13 \text{ nm}^3$ . This number follows assuming  $a \approx (0.5 \text{ nm})^2$  and  $d \approx 0.5 \text{ nm}$ . The value used for the activation length  $d$  is motivated in detail in the Appendix. Numerical values for  $q$  are discussed in the next section in the context of a specific experimental system. The activation energy  $e$  is also adjustable, but only within bounds. Its upper limit is the potential well depth of the breaking covalent bond. It may be lower, but should not be smaller than the typical physical interaction energies between polymer and filler.

Next we turn to  $\langle n \rangle$ , which is the probability that a chain is load-bearing. The cartoon in Fig. 1 illustrates how LBCs can arise in the presence of filler particles. When the sample

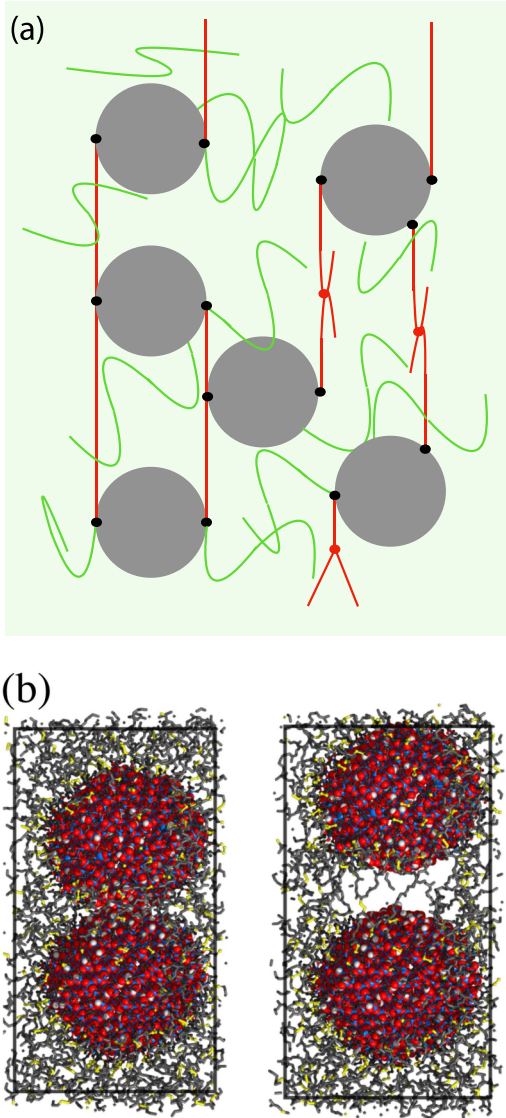


FIG. 1. (a) Cartoon of filler particles (shaded circles) inside an elastomer close to its breaking stress. The red line illustrate polymer LBCs or rather chain segments. The green lines are chains which do not carry much load. Dots indicate anchoring sites on the particle surface (black dots) or chemical or physical crosslinks (red dots). (b) Snapshot from an atomistic computer simulation studying the interaction between two silica particles tied to a surrounding polyisoprene matrix via short silanes (taken from Ref. [24]). Notice the void space appearing between the particles as they are pulled apart keeping one particle stationary while the other experiences a force acting on its center of mass.

is stretched, particles previously in close proximity are separated, creating voids between them. This is shown explicitly in a picture from a computer simulation. Two silica particles are embedded in a crosslinked polyisoprene matrix. One of the particle is kept stationary while its neighbor is pulled away. As a result a void space appears between the two particles. Even though typical rates (of motion) in atomistic computer simulations are fast compared to the rates used in mechanical testing, the polymer matrix will not be able to flow around the particles and close the void due to crosslinking (typical mesh

sizes in most technically relevant elastomers are comparable to the dimension of the particles). The “walls” of the tubelike voids will contain several LBCs. The existence of several LBCs instead of just one or perhaps none is favored by two circumstances: (1) The walls of the voids present the polymer chains with increased conformational freedom compared to the bulk polymer. (2) The chain monomers attached to the equatorial regions of the particles can slip without being lifted out of the adsorption potential. This allows a concerted load uptake of several chains around the equator without breaking them or lifting them away from the particle surface before their partners have become load-bearing. In detail this depends on the surface morphology of the particles and on the type of bond between particle surface and polymer. Note also that ideas along these line have been formulated before by Dannenberg (for a summary see Sec. 9.4.3.2 of Ref. [5]).

In the following we divide the chains (or chain segments) into those which are “slack” and those which are “tight” or load-bearing. Note that each of those chain segments is anchored on both ends either by crosslinks or via adsorption on a filler particle surface. The overall number of LBC segments  $N$  is given by  $N = \sum_i n_i$ , where the sum is over all chain segments and  $n_i = 1$  if  $i$  is load-bearing and zero otherwise. The total energy of the LBC is given by  $E = \sum_i \epsilon_i n_i$ , wherein  $\epsilon_i = 0$  if  $i$  is not load-bearing, i.e., the slack chains define the zero of this energy scale. The partition function of the LBC segments is  $Q = \sum_{n_1, n_2, \dots} \exp[-\beta \sum_i (\epsilon_i - \mu) n_i]$ , where  $\mu$  is their chemical potential and  $\beta = 1/(RT)$ . In essence we utilize an open system in terms of the total number of LBCs. This  $Q$  can be rewritten as  $Q = \prod_i \sum_n \exp[-\beta(\epsilon_i - \mu)n]$ , where  $n = 0, 1$  and  $Q = \prod_i (1 + \exp[-\beta(\epsilon_i - \mu)])$ . The final result then follows via  $\langle n_j \rangle = \partial_{(-\beta\epsilon_j)} \ln Q$ . For the sake of simplicity we make the approximation that all LBCs possess the same  $\epsilon_i$  equal to  $\epsilon$ . Hence we obtain

$$\langle n \rangle = \frac{1}{\exp[(\epsilon - \mu)/RT] + 1}. \quad (5)$$

It is useful to consider this calculation and its result in the context of a different but largely analogous physical problem, i.e., adsorption of molecules (from a gas phase) onto a surface. Here an empty adsorption site corresponds to a slack chain segment, whereas an occupied adsorption site corresponds to a LBC. If we distribute  $M$  noninteraction indistinguishable molecules on  $M_o (> M)$  adsorption sites, i.e., the coverage is  $\theta = M/M_o$ , then the canonical partition function of the adsorbed molecules is  $Q = q(T)^M M_o! / [(M_o - M)! M!]$ . The quantity  $q(T) = \exp[-\beta\epsilon_a] q_s(T)$  is the single molecule partition function, where we have split off the factor containing the adsorption energy  $\epsilon_a$ . Using Stirling’s approximation we obtain the molecule’s chemical potential via  $\beta\mu = -\partial \ln Q / \partial M = \ln \frac{\theta}{(1-\theta)q(T)}$ . Solving this equation for  $\theta$  we find  $\theta = \frac{1}{\exp[(\epsilon_a - \mu)/RT] + 1}$ , where we have set  $q_s(T) = 1$  (alternatively we may adsorb  $q_s(T)$  into an effective  $\epsilon_a$ ). The functional form of this equation is identical to that of Eq. (5). In the case if adsorption, however, chemical equilibrium allows to replace  $\mu$  by the gas phase chemical potential which yield the adsorption isotherm  $\theta = \theta(P)$ , where  $P$  is the gas pressure [of course,  $q_s(T)$  in this case not just unity but depends on the thermally excited degrees of freedom of the

adsorbed molecules]. Nevertheless, in a rough sense, the role of pressure in the case at hand is assumed by quantities like the filler or the crosslink concentration. Moreover,  $\epsilon_a$  usually is a function of temperature  $T$  if the molecule-surface interaction involves molecular groups on the surface (e.g., silanol groups or flexible moieties) possessing thermally excited degrees of freedom.  $\epsilon$  in Eq. (5) also is contributed by many atoms along a LBC, and consequently we expect  $\epsilon = \epsilon(T)$ . It seems reasonable to invoke equipartition and thus  $\epsilon = \epsilon_o T$ , where  $\epsilon_o$  is a constant, appears to be a reasonable form.

But what is the chemical potential? The chemical potential should depend on temperature too of course. In addition we shall assume that it also depends on the concentration of anchoring sites able to support excited chain segments. Anchoring sites can be surface sites or surface bonds due to filler particles dispersed in the polymer matrix and, of course, physical or chemical crosslinks in the polymer matrix. Hence,  $\mu = \mu(T, n_s, n_c)$ , where  $n_s$  denotes the volume number density of anchoring sites on particle surfaces within the system and  $n_c$  refers to the polymer crosslink density in the system. Increasing  $n_s$  as well as  $n_c$ , at least initially, will lead to an increase of the work required for LBC formation, because of the increasing stiffness of the material. Formation of a LBC also requires the proximity of two anchoring sites. The probability for this to happen is roughly proportional to  $(n_s + \lambda(n_c)n_c)^2$ , where  $\lambda(n_c)$  is an additional function of  $n_c$ . When  $n_c$  is not too large, we expect that  $\lambda(n_c)$  is close to unity. There may be a difference in their relative weight distinguishing surface anchoring sites from crosslinks—but this is ignored for now. When  $n_c$  increases we expect that the work, which must be invested to produce a LBC, is reduced due to an overabundance of crosslinks. This we model by the simple approximate form  $\lambda(n_c) = 1 - n_c/n_{c,o}$ .  $n_{c,o}$  is a certain threshold density beyond which the aforementioned reduction of the work required to produce a LBC becomes significant. No such factor is introduced in the case of  $n_s$ . This is because the formation of LBC is tied to the motion of the particle as a whole rather than the “tightening” of a single short chain segment between two crosslinks. However, addition of particles reduces the tensile strength by creating excluded volume for possible LBCs, and this is accounted for by the factor  $(1 - \phi)$  in Eq. (1). Hence we assume that the chemical potential is of the form

$$\mu = \mu(T, n_s, n_c) = \mu_o(T)[n_s + \lambda(n_c)n_c]^2. \quad (6)$$

Note that  $n_s = A_s/(a_s V)$ , where  $A_s$  is the total filler surface area in the volume  $V$  and  $a_s$  is the effective area of an anchoring site. If  $N_p$  is the total number of particles, we may express the filler volume fraction via  $\phi = N_p v_p/V$ , where  $v_p$  is the volume of a filler particle. In addition,  $A_s = N_p a_p$ , where  $a_p$  is a filler particle’s surface area. Assuming that the particles are spheres of uniform diameter  $d_p$  we obtain

$$\mu = \epsilon_o T \left( \frac{\phi + \Omega}{\phi_c} \right)^2, \quad (7)$$

where  $\Omega = v_o n_c (1 - n_c/n_{c,o})$ ,  $\phi_c = \sqrt{\epsilon_o T / \mu_o(T)} v_o$  and  $v_o = (a_s d_p / 6)$ . Equation (5) therefore becomes

$$\langle n \rangle = \frac{1}{\exp[(\epsilon_o/R)(1 - (\phi + \Omega)^2/\phi_c^2)] + 1}. \quad (8)$$

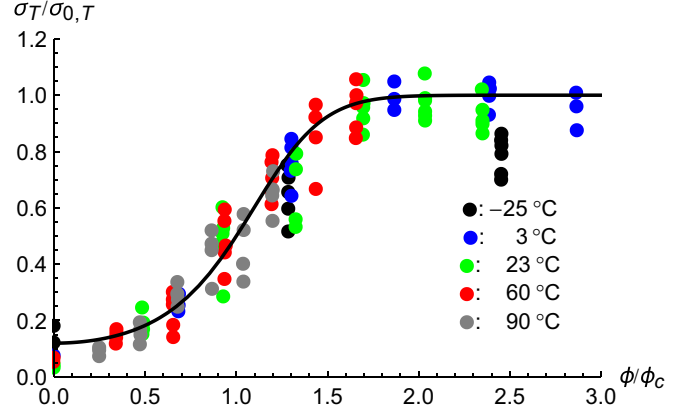


FIG. 2. Master curves obtained for his data points by Plagge [15] in comparison to Eq. (8) (solid line) for  $\epsilon_o/R = 2.0$  and  $\Omega = 0$ .

It is worth noting that  $\phi$  here appears in the argument of an exponential function. This is different from how  $\phi$  enters into theories for the dynamic moduli describing hydrodynamic “reinforcement” or the “reinforcement” beyond the filler percolation threshold in the context of the Payne effect [19,25]. In particular it signals a distinctly different reinforcement mechanism underlying tensile strength. In the former case the mechanical behavior of the dynamic moduli of filled elastomers is often described based on load-bearing paths composed of filler particles agglomerates and their networks enveloped in sheaths of polymer traversing a bulk polymer matrix [26]. At large amplitudes it appears that the load-bearing capability of individual chain segments becomes the key element governing a composite’s strength. This idea was also the basis of Bueche’s considerable theoretical work on tensile strength (cf. the introduction). Despite this similarity, however, he followed a conceptual path very different from the present.

### III. A FIRST COMPARISON TO EXPERIMENTAL DATA

Figure 2 depicts master curves obtained from tensile strength measurements by Plagge [15] in comparison to Eq. (8). Data points at the indicated temperatures are obtained via tensile tests of EPDM (Keltan 4450) filled between 10 to 60 phr (parts per hundred rubber by weight) with CB (N339). The vulcanization system consisted of 1.05 phr sulfur and 1.40 phr N-cyclohexyl-2-benzothiazole sulphenamide (CBS). The data are scaled horizontally, using the inflection points of the apparently s-shaped curves. Plagge finds empirically that  $\phi_c = c_o(T - T^*)$ , where  $T^* \approx -50^\circ\text{C}$  can essentially be equated with the glass temperature and  $c_o \approx 1.26 \times 10^{-3} \text{ K}^{-1}$ . Note that this implies

$$\mu_o(T) = \epsilon_o T \left[ \frac{v_o}{c_o(T - T^*)} \right]^2, \quad (9)$$

i.e., the work necessary to excite a LBC in terms of a stretched chain segment increases as  $T$  approaches  $T^*$ , which appears reasonable. Of course, the chemical potential cannot diverge and has to be continuous on both sides of  $T^*$ . But this theory is expected to be replaced by one build around a different rupture mechanism near the glass transition. The vertical shift uses

the apparent plateau value of the tensile strength. The data do show, of course, a reduction of the tensile strength in the limit of high filler concentration in accordance with the standard observation. But this reduction, compared to the overall scatter, is rather weak in the filler range considered here, i.e., a “plateau value” is asserted with reasonable accuracy, and therefore we shall ignore the excluded volume factor  $(1 - \phi)$  for now.

To good approximation the theoretical description of the reduced data is Eq. (8). However, Eq. (8) depends not only on  $\phi/\phi_c$  but also on  $\Omega/\phi_c$ . Since  $\phi_c$  depends on temperature,  $\langle n \rangle$  vs  $\phi/\phi_c$  is going to be different for each temperature unless  $\Omega = 0$ . A comparison of Eq. (8) with the mastered data is included in Fig. 2 using  $\epsilon_o/R = 2.0$  and  $\Omega = 0$  (solid line). The line is in very good accord with the data. But is  $\Omega \approx 0$  justified? As we shall see below,  $\phi_c$ , for the present data set, is in the range  $0.2 > \phi_c > 0.025$ . Neglect of  $\Omega/\phi_c$  compared to  $\phi/\phi_c$  requires  $\phi/\phi_c \gg \Omega/\phi_c$ . From Fig. 2 we see that the smallest value of  $\phi/\phi_c$  for which there are data points is 0.25 ( $\phi/\phi_c = 0$  must be excluded since the scaling does not apply to the unfilled system.). Thus we must require  $0.25 = \phi/\phi_c \gg \Omega/\phi_c$  or  $0.25\phi_c \gg \Omega$  or, inserting the lower bound of the  $\phi_c$  range,  $5 \times 10^{-3} \gg \Omega$ . With  $a_s \approx 0.25 \text{ nm}^2$ ,  $d_p \approx 50 \text{ nm}$ , and  $n_c \approx 360 \text{ mol/m}^3 \approx 0.22 \text{ nm}^{-1}$  [27] one has  $\Omega \approx 0.46(1 - 0.22/n_{c,o})$ . Combining this with the previous condition on  $\Omega$  we conclude  $n_{c,0} \approx n_c$ . This is not unreasonable because the crosslink density  $n_c$  is already quite high. However,  $\Omega$  is not a sensitive parameter in the first place. Using, for instance,  $\Omega/\phi_c = 0.1$  merely shifts the solid line by the width of the symbols to the left. Finally note that the value  $\epsilon_o/R = 2$  used to fit the master curves with Eq. (8) indicates that  $\epsilon$  corresponds to the energy of about two fully excited vibration modes.

Figure 3 illustrates the application of Eq. (4) to Plagge’s data (solid circles) in the apparent plateau regime, i.e., Eq. (1) reduces to  $\sigma_T = \sigma_{T,o}(1 - \phi)$  (here  $\phi$  is set to 0.2), where  $\sigma_{T,o} = RT_o v s$  and  $T = T_o t$ . The theoretical fits (black lines) are for these data. The three curves represent different parameter sets—dashed line: solution of Eq. (4) for  $e = 17.5$  ( $E_b = 40 \text{ kJ/mol}$ ),  $c = 13.2$ , and  $q = 4$ ; solid line: solution of Eq. (4) for  $e = 35$  ( $E_b = 80 \text{ kJ/mol}$ ),  $c = 25.5$ , and  $q = 9$ ; dotted line: solution of Eq. (4) for  $e = 66$  ( $E_b = 150 \text{ kJ/mol}$ ),  $c = 46.5$ , and  $q = 18$ . The variation of  $E_b$  is motivated by different types of bonds. The highest value,  $E_b = 150 \text{ kJ/mol}$ , represents measurements of the dissociation energy of the tetrasulfide linkages in dimethyl tetrasulfide via thermal decomposition [28]. The lower values cover the range of physical bonds involving several monomer units on CB. Litvonov *et al.* [29] have studied the interaction of EPDM (K4802) with various grades of CB (N550, N330, N115) using low-field proton NMR. They conclude that the thickness of the immobilised EPDM-CB interface layer is about (and perhaps slightly greater than)  $0.6 \text{ nm}$  ( $0.6 \text{ nm}$  is about one chain diameter) and the average number of C–C bond per adsorption site is approximately 18. Schröder [30], in his gas adsorption measurements of  $\text{C}_2\text{H}_4$  on CB, observes adsorption energies between 15 to 25 kJ/mol. The low energy corresponds to the basal plane whereas higher energies occur at steps and in corners. However, the 15 kJ/mol sites are the most frequent—even on CB. In combination with the NMR work this means

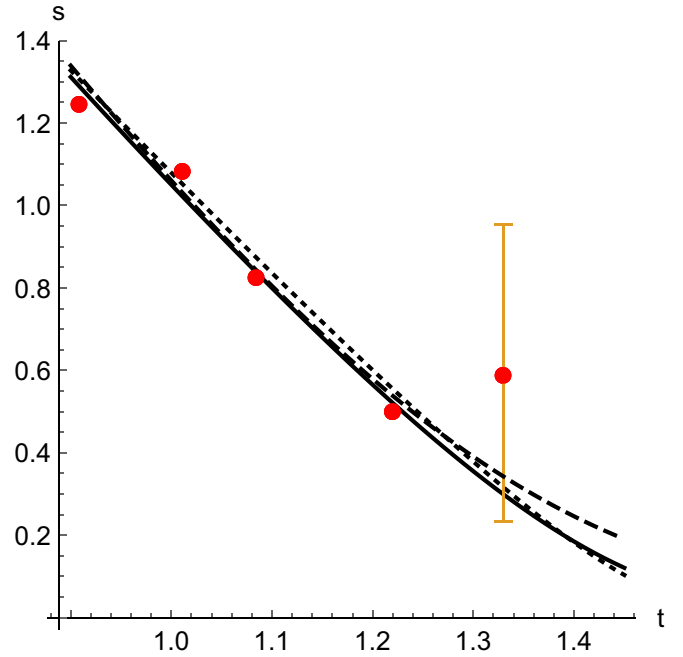


FIG. 3. Temperature dependence of the tensile strength (hollow circles) in the plateau regime obtained by Plagge. Here  $s = \sigma_{T,o}v/(RT_o)$  and  $t = T/T_o$ . The solid circles follow from the hollow circles after subtracting the respective tensile strength for  $\phi = 0$ . The error bars, except in the case of the one shown explicitly, are comparable to the size of the circles. Dashed line: solution of Eq. (4) for  $e = 17.5$  ( $E_b = 40 \text{ kJ/mol}$ ),  $c = 13.2$ , and  $q = 4$ ; solid line: solution of Eq. (4) for  $e = 35$  ( $E_b = 80 \text{ kJ/mol}$ ),  $c = 25.5$ , and  $q = 9$ ; dotted line: solution of Eq. (4) for  $e = 66$  ( $E_b = 150 \text{ kJ/mol}$ ),  $c = 46.5$ , and  $q = 18$ .

that the “adsorption site” energy may be comparable to the aforementioned dissociation energy, but it is likely, due to the short range of the adsorption potential [31], that not all of the 18 C–C bonds will possess the optimal separation from the surface and that this will reduce the overall adsorption energy of the polymer segments. Note that none of the  $E_b$  values is ruled out by the comparison of theory and experiment. However, the local stress enhancement factor  $q$ , introduced above, is quite large (and perhaps excessively large) when  $E_b = 150 \text{ kJ/mol}$  (increasing  $E_b$  increases the slope of the fit and a larger value of  $q$  is needed to counteract this).

Figure 4 shows an overall comparison of Eq. (1) to the measured tensile strengths. Here the temperature dependence is affected not only by  $\sigma_{T,o}$  via Eq. (4) but also by the chemical potential in  $\langle n \rangle$  via Eq. (8). The overall agreement between theory and experimental data is quite encouraging. The only significant deviation is for  $-25^\circ\text{C}$ . As stated before, this theory will break down near the glass temperature (here approx.  $-47^\circ\text{C}$  [15]), i.e. the underlying concept of individual LBC stretched between anchoring points loses its validity.

#### IV. COMPARISON TO OTHER MEASUREMENTS AND DISCUSSION

Comparison of the theory with experimental data requires considerable knowledge about the system (crosslink density,

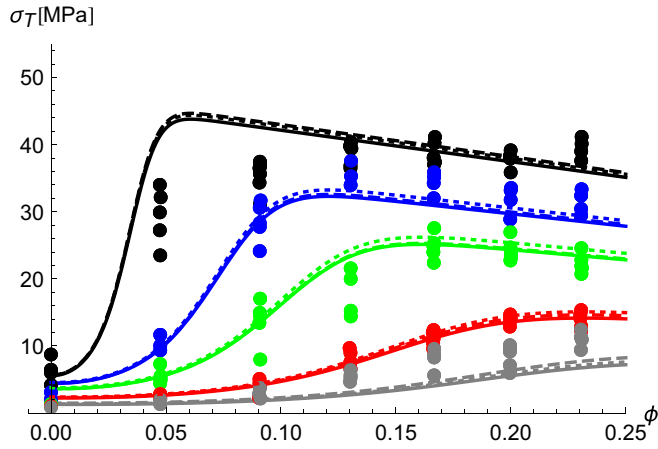


FIG. 4. The symbols depict measured tensile strengths  $\sigma_T$  vs filler volume fraction  $\phi$  at a series of temperatures  $T$  (gray: 90 °C, red: 60 °C, green: 23 °C, blue: 3 °C, and black: -25 °C) taken from Ref. [15]. The data are the same as the data depicted in the master representation of the measurements in Fig. 2 using corresponding colors. The solid lines show the comparison of the experiment to Eq. (1) for the three parameter sets obtained via the data points in Fig. 3 (line types correspond).

filler type (important for judging the value of  $E_b$ ), filler content, particle size, temperature, etc.). This information is not always available in its entirety and therefore the following is qualitative.

*The effect of particle size:* Fig. 5(a) depicts the theoretical prediction of a hypothetical experiment based on two temperatures in Fig. 4. The curves are obtained via Eq. (1) where  $\phi$  is replaced by  $\phi D_{N339}/D$ . For  $D = D_{N339}$  the curves coincide with the  $E_b = 40$  kJ/mol results of the same color, i.e., temperature, in the previous figure at  $\phi = 0.1$  (solid) and  $0.2$  (dashed). For  $D \neq D_{N339}$  the curves illustrate the variation of the aggregate or particle size. Generally the tensile strength decreases with increasing  $D$ . Note that the diameter of N339 aggregates is roughly 70 to 80 nm [32]. At small particle size the theoretical results indicate a saturation value for  $\sigma_T$ . Where this occurs depends on temperature and volume fraction and, presumably, on the system itself. Nevertheless, curves like these, a number of them featuring a plateau in the small aggregate limit, have been observed by Sambrook [33], who studies the influence of temperature and filler type on the tensile strength of CB filled vulcanizates of NR and SBR. Unfortunately, he presents these data as quasi-3D plots, which prevents a reliable extraction of the data. The measurements (red dots) in Fig. 5(b) are taken from Fig. 10.15 in Ref. [5]. This figure depicts the tensile strength for a series of silicon rubber compounds filled with 38 phr (roughly  $\phi \approx 0.12$ ) of silica with different surface areas. The surface areas were converted to particle sizes using Table V in Ref. [16]. A rough qualitative fit of the present theory to the resulting data is accomplished by using the position of the step, which the measured tensile strengths clearly exhibit, to define a reference size  $D_{ref}$ . In this case the previous approximation  $\Omega \approx 0$  does not suffice. The corresponding result is the dashed line, i.e., here  $\Omega > 0$  is necessary. Nevertheless, the theory appears

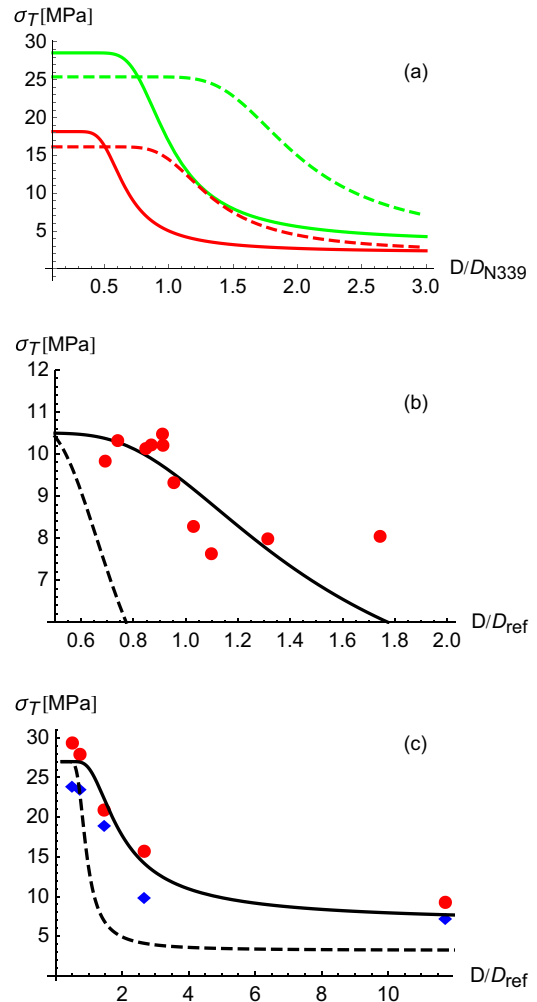


FIG. 5. (a) Tensile strength  $\sigma_T$  vs particle size relative to N339. The curves correspond to the theoretical results for  $T = 60$  °C (green) and 23 °C (red) at  $\phi = 0.1$  (solid lines) and  $\phi = 0.2$  (dashed lines) shown in the previous figure. (b) Measurements (red dots) taken from Fig. 10.15 in Ref. [5]. This panel depicts the tensile strength for a series of silicon rubber compounds filled with 38 phr of silica with different surface areas, which here are converted to particle size. (c) Tensile strength  $\sigma_T$  vs particle size relative to N220 in an SBR vulcanizate. The data points are taken from Fig. 4 in Ref. [13] [40 (red spheres) and 30 (blue diamonds) phr].

to drop below the measured values for the larger particles in the experimental range. Another experimental example for the effect of particle size on tensile strength in a CB-filled SBR vulcanizate is depicted in Fig. 5(c). The data points are taken from Fig. 4 in Ref. [13]. The reference particle size here is that of N220. The parameter  $\epsilon_o/R$  is the same as in the two previous panels. All other parameters are within a factor of two compared to the measurements discussed in the previous section. Note that the  $\sigma_T$  in the limit  $d_p \rightarrow 0$  is adjusted between the apparent limiting values of the two data sets, i.e., the shape of the theoretical curve is due to  $\langle n \rangle$  alone. As in Fig. 5(b) the approximation  $\Omega \approx 0$  does not suffice (dashed line) and the polymer crosslink density must be included, i.e.,  $\Omega > 0$  is necessary (solid line).

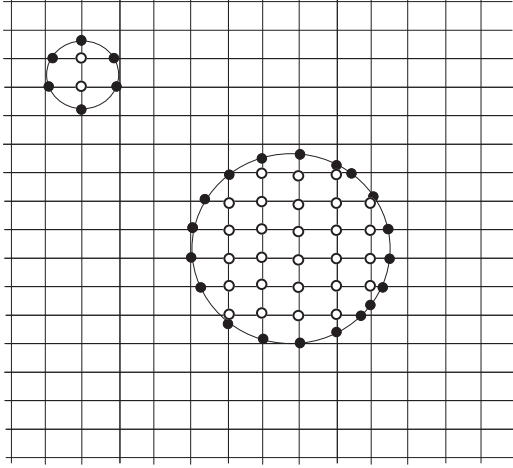


FIG. 6. Open circles: bulk crosslinks; solid circles: surface bonds. The ratio of displaced bulk crosslinks to surface bonds is 2/5 for the small circle but 27/19 for the large circle.

In this context it is worth mentioning another study in the literature, discussing the tensile strength of polymer composites. In Ref. [34] the authors observe a “transition” from an increase of the tensile strength to its reduction as function of filler volume fraction depending on the size of the filler particles. The increase is observed when the particles are small ( $\sim 0.01 \mu\text{m}$ ), while a decrease is observed when the particles are large ( $> 0.1 \mu\text{m}$ ). The present theory does not apply to large particle size, because there is a limit to the validity of (7) when  $d_p$  becomes large ( $\sim \mu\text{m}$ ). [The two data points at  $D/D_{\text{ref}} \approx 12$  in Fig. 5(c) are most likely already borderline cases.] The idea why this is so is depicted in Fig. 6. The gridlines correspond to a crosslinked polymer network. When  $D$  is small the particles displace few crosslinks in the polymer network (open circles) in comparison to the anchoring sites they provide on their surface (filled circles). When  $D$  grows this changes, because the number of replaced crosslinks scales with  $D^3$  whereas the number of anchoring sites scales with  $D^2$ .

It is instructive to briefly consider this macroscopic limit using linear theory of elasticity. The problem is that of a rigid sphere embedded inside of an elastic matrix subject to a tensile stress  $\sigma_{zz}$  in the  $z$  direction. The excess elastic free energy density  $F_{el}/V$  in a sample containing noninteracting (or very diluted) rigid spheres at a volume fraction  $\phi$  is given

$$\frac{F_{el}}{V} = \frac{\sigma_{zz}^2}{2E} \left( 1 + \frac{\phi}{2} \right), \quad (10)$$

where  $E$  is the matrix’s elastic modulus (see, for instance, Ref. [35]). This formula is a result *en route* to Smallwood’s expression describing the enhancement of the modulus of an elastic matrix by the addition of spherical particles. Note that Eq. (10) is derived assuming an ideal (no detachment, no slip) boundary between the matrix and the particle. This is a macroscopic theory, which does not contain or require a molecular description of the matrix-particle interface. Following the guiding principle that the propagation of a crack requires energy stored in the material, we can replace  $F_{el}/V$

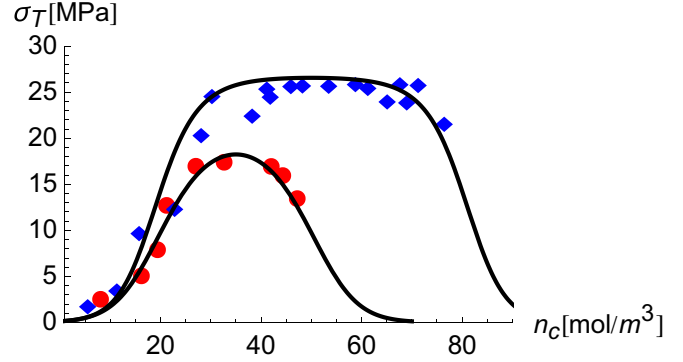


FIG. 7. Tensile strength  $\sigma_T$  vs crosslink density  $n_c$ . Fit of the present model (solid lines) to data from Figs. 1 and 3 in Ref. [38]. The systems are SBR 1006 (red circles) and SBR 1500 (blue diamonds) containing 30 phr of HAF black.

by a critical elastic energy density  $e_c$  and simultaneously  $\sigma_{zz}$  by  $\sigma_T$ . Using  $E \propto n_c$  and  $\phi \ll 1$  yields

$$\sigma_T \sim n_c^{1/2} (1 - \phi/2). \quad (11)$$

Qualitatively this predicts a decrease of  $\sigma_T$  with  $\phi$  and an increase with crosslink density. However, even in this regime of large particles (several hundred  $\mu\text{m}$ ) a strong dependence on particle diameter is possible [36], which this simple theoretical argument, probably due to its unrealistic boundary conditions (cf. Ref. [37]), does not capture.

*The effect of crosslinks:* As an example we compare to measurements of the tensile strength vs polymer crosslink density published by Büche [38]. The systems are sulfur vulcanizates of SBR 1006 and SBR 1500 containing 30 phr of HAF (high abrasion furnace) black. The comparison with the present theory is shown in Fig. 7. The shape of  $\sigma_T$  vs  $n_c$  is governed by  $\langle n \rangle$ , i.e., this mainly is a test of the LBC occupation number as a function of crosslink density. Due to the lack necessary information (temperature) we merely adjust  $\sigma_{T,o}$  to match the experimental peak height for SBR 1006. (In general we expect some dependence of  $q$  on the crosslink density however.) Here  $\phi/\phi_c \approx 0.68$  is kept constant ( $\phi \approx 0.15$ ). In addition  $v_o$  is about three times larger than the value used in the last section and  $\epsilon_o/R \approx 10$ . The threshold crosslink density  $n_{c,o}$  is  $\approx 70 \text{ mol m}^{-3}$  for SBR 1006 and  $\approx 100 \text{ mol m}^{-3}$  for SBR 1500. In other words, the two theoretical curves differ only in their values for  $n_{c,o}$ ! Note in particular that this one polymer-specific parameter adjustment not only yields the correct change of the peak height but also produces a change of the peak shape in accord with the measurements.

*Strain rate dependence:* Tensile strength, in general, is strain rate dependent. The present theory applies in the limit of small strain rates. Early work by Smith [39] on SBR vulcanizates already shows that over a wide range of strain rates  $k_s$ , above a certain threshold and below the range when the sample becomes glassy, the approximate relation  $\sigma_T(1)/\sigma_T(2) \approx k_s(2)/[k_s(1)]^\alpha$  with  $\alpha > 0$  is satisfied. Here (1) and (2) refer to two different rates. This means that if the strain rate increases so does the tensile strength.

In Eq. (4)  $q(> 1)$  accounts for the plausible expectation that the stress on an individual LBC is larger than the macroscopic tensile stress on the sample. Thus,  $q$  should in fact

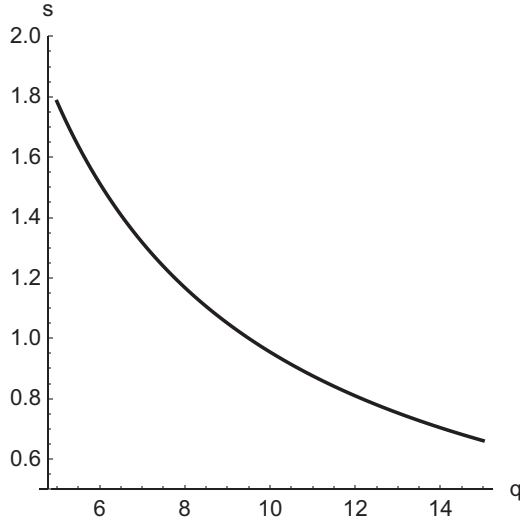


FIG. 8.  $s$  vs  $q$  according to Eq. (4). The other parameter values are the same as for the solid line in Fig. 3. Here  $t = 1$ .

depend on time, i.e.,  $q = q(t)$ . This is because the system will redistribute the applied load during its approach towards an equilibrium distribution of the internal stress (an early paper discussing the significance of the equilibrium stress distribution in the context of filled rubbers is Ref. [40]). Increasing the strain rate reduces the extend of the internal relaxation, which means a less inhomogeneous stress distribution, which in turn means a smaller  $q$ . Hence we expect (very roughly)  $q \sim k_s^{-\beta}$  ( $\beta > 0$ ), i.e.,  $\sigma_{T,o}$  should increase as  $q$  decreases. This is indeed the case as shown in Fig. 8.

The effect of strain rate on tensile strength depends greatly on whether the rubber is filled or not, on crosslink density, polymer type, etc. [41–43]. Probably it is fair to state that despite the many years which have passed since these observations were made, there still is no real understanding (molecular theory), apart from phenomenological ideas usually centered on the Williams-Landel-Ferry shift factor.

## V. CONCLUSION

The unique element in this theory of rubber tensile strength is the Fermi probability of LBCs  $\langle n \rangle$ , which contains the dependence on filler volume fraction (aside from a multiplicative excluded volume factor), particle size and polymer crosslink density. The description of the temperature is shared with  $\sigma_{T,o}$ , an effective single chain tensile strength calculated using Eyring’s theory. The theory appears to be in very good qualitative accord and, depending how much is known about the system, also in semiquantitative agreement with the experiments. In particular the dependence of tensile strength on particle size (at least for active fillers) has been integrated into a theory for elastomer tensile strength. Since all parameters in the model do have a physical meaning, it is, in principle, possible to study their collective and interdependent effect on rubber tensile strength. It is the hope of the author that this can be of use to rubber material developers in their quest to target selected performance parameters for improvement while keeping others from causing the opposite. Nevertheless,

a full understanding of both strength and elongation at break requires the ability to calculate failure envelopes [5] including their dependence on crosslinking, filler volume fraction, filler type, temperature, and possibly more. With the model presented here this is not yet possible.

## ACKNOWLEDGMENT

I am indebted to Dr. Jan Plagge for numerous discussions on the subject and for his permission to use his experimental data prior to their publication.

## APPENDIX: ACTIVATION LENGTH

The following is a discussion of the “activation length”  $d$  and a motivation for its value in this model. The concept of an activation length can be studied by modeling the thermal dissociation of a simple model polymer—a Morse chain.

The latter consists of the linear catenation of  $N$  beads, interacting via Morse potentials  $V(r) = D[1 - \exp(-a(r - r_o))]^2$  between neighboring beads. The quantity  $D$  is the depth of the potential minimum at  $r_o$ . This potential is harmonic near the bottom,  $V(r) \approx Da^2(r - r_o)^2$  ( $r \approx r_o$ ), but has a finite depth. If the force on a pair of neighboring beads exceeds  $aD/2$  the link will break. The chain is thermalized using Langevin dynamics,  $\ddot{\vec{r}}_i = \vec{F}_i + \vec{Z}_i - \zeta \dot{\vec{r}}_i$  (each bead possesses unit mass). Here  $\vec{F}_i$  is the force on bead  $i$ , which for every bead between  $i = 2$  and  $i = N - 1$  is the combined force due to the Morse bonds with its two neighbors. The terminal beads experience one Morse interaction, because they possess one neighbor only, plus a constant tensile force  $f_p (\geq 0)$  in the  $-z$  direction in case of  $i = 1$  and the  $z$  direction in the case of  $i = N$ . The  $\vec{Z}_i$  are Gaussian random forces satisfying  $\langle \vec{Z}_i(t) \cdot \vec{Z}_j(t') \rangle = 6\zeta T \delta(t - t') \delta_{ij}$ , where  $\zeta$  is a friction parameter.

We simulate chain between  $N = 2$  to  $N = 100$  for a series of temperatures. For each temperature we determine the frequency of chain dissociation  $h_{\text{break}}(T)$ . A chain is considered to be dissociated if at the end of the simulation there exists at least one bond with a length  $\geq 5r_o$  (here we set  $r_o = 1$ ). Other multiples of  $r_o$ , e.g.,  $4r_o$  or  $6r_o$ , work just as well, i.e., the dissociation criterion is not a sensitive parameter. However, since the activation length  $d$  is found to be around  $4r_o$  (cf. below), it is reasonable to use a factor multiplying  $r_o$  which is (slightly) larger than 4. Figure 9(a) shows  $h_{\text{break}}(T)$  vs temperature  $T$  for  $N = 10$  ( $a = 1$ ,  $D = 0.6$ ,  $f_p = 0$ , and  $\zeta = 0.1$ ). Each simulation run encompasses  $2 \times 10^6$  time steps with the length 0.0025.  $h_{\text{break}}(T)$  is computed from 10 independent runs at the same temperature. Figure 9(b) shows the temperature  $T_{\text{break}}$  at which chain rupture occurs [inflection point of the fit to  $h_{\text{break}}(T)$ ] for  $N$  between 2 and 100. The error bars indicate the width of the step.

There are two main results: (1)  $T_{\text{break}} \approx 0.1$  when  $f_p = 0$ , i.e.,  $D/T_{\text{break}} \approx 10$  (note that in these units  $k_B = 1$ ). This result is not altered significantly by changing  $a$  or  $\zeta$  as indicated. (2) Increasing  $f_p$  from 0 to 0.1 lowers  $T_{\text{break}}$  significantly. The same reduction of  $T_{\text{break}}$  in comparison to the standard case ( $D = a = 1$ ) is obtained if  $f_p = 0$  but  $D \approx 0.6$ . This means that in the present case the “activation length”  $d \approx 4$  (or  $4r_o$ ), which follows via  $D - f_p d = D'$  with  $D = 1$ ,  $f_p = 0.1$  and  $D' = 0.6$ . Overall this is a crude argument, but it

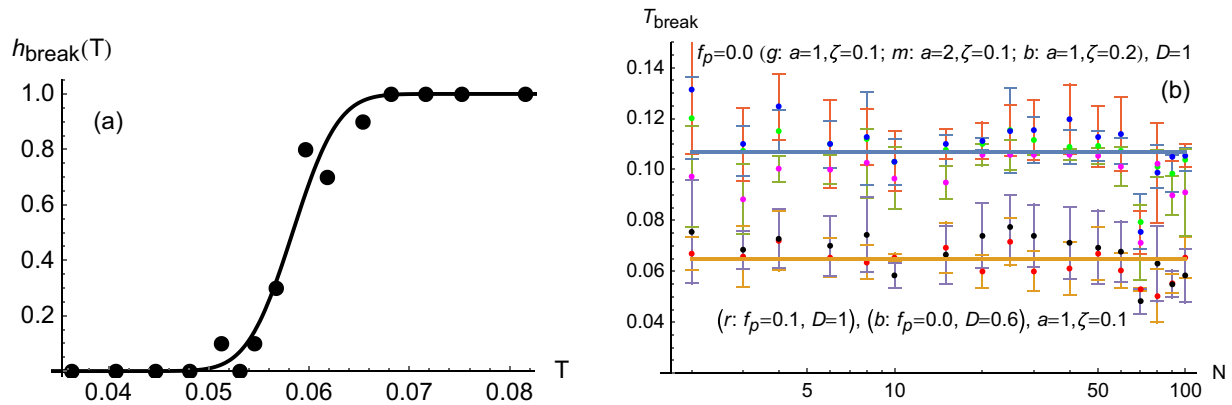


FIG. 9. (a) Frequency of chain break  $h_{\text{break}}(T)$  vs temperature  $T$  for  $N = 10$  ( $a = 1$ ,  $D = 0.6$ ,  $f_p = 0$ , and  $\zeta = 0.1$ ). (b) Chain rupture temperature  $T_{\text{break}}$  for  $N$  between 2 and 100 for different parameter values. The letters g, m, b, r, and b stand for the colors of the dots (green, magenta, blue, red, and black) distinguishing the indicated parameter sets. Horizontal lines are a guide for the eye.

shows that the “activation length” is on the order of perhaps several equilibrium bond lengths and not, for instance, tied to the chain length. The same conclusion was reached by other means in a recent paper studying the fracture of vitrimers [44].

We want to close this digression with a short comment on the above ratio  $D/T_{\text{break}} \approx 10$ . The temperature at which the

chains dissociate does depend on the details of the partition functions in the two sides of the reaction as well as on the reaction path. Since our chain is merely a simple model, one should not expect find this ratio for real polymers. However, quite generally it is observed that the thermal energy  $k_B T_{\text{break}}$  is considerable less than what one expects from the mere depths of the bond potentials.

- [1] F. Bueche, The tensile strength of elastomers according to current theories, *Rubber Chem. Technol.* **32**, 1269 (1959).
- [2] F. Bueche and J. C. Halpin, Molecular theory for the tensile strength of gum elastomers, *J. Appl. Phys.* **35**, 36 (1964).
- [3] *Reinforcement of Elastomers*, edited by G. Kraus (Interscience Publishers, New York, 1965).
- [4] E. M. Dannenberg, The effects of surface chemical interactions on the properties of filler-reinforced rubbers, *Rubber Chem. Technol.* **48**, 410 (1975).
- [5] M.-J. Wang and M. Morris, *Rubber Reinforcement with Particulate Fillers* (Hanser Verlag, Cincinnati, 2021).
- [6] S. C. Peterson, Carbon black replacement in natural rubber composites using dry-milled calcium carbonate, soy protein, and biochar, *Processes* **10**, 123 (2022).
- [7] C. G. Robertson and N. J. Hardman, Nature of carbon black reinforcement of rubber: Perspective on the original polymer nanocomposite, *Polymers* **13**, 538 (2021).
- [8] C. G. Robertson, L. B. Tunnicliffe, L. Maciag, M. A. Bauman, K. Miller, C. R. Herd, and W. V. Mars, Characterizing distributions of tensile strength and crack precursor size to evaluate filler dispersion effects and reliability of rubber, *Polymers* **12**, 203 (2020).
- [9] C. Neogi, A. K. Bhowmick, and S. P. Basu, Threshold tensile strength and modulus of carbon-black-filled rubber vulcanizates, *J. Mater. Sci.* **25**, 3524 (1990).
- [10] S.-S. Choi, B.-H. Park, and H. Song, Influence of filler type and content on properties of styrene-butadiene rubber (SBR) compound reinforced with carbon black or silica, *Polym. Adv. Technol.* **15**, 122 (2004).
- [11] S. Dai, G. Ao, and M.-S. Kim, Reinforcement of rubbers by carbon black fillers modified by hydrocarbon decomposition, *J. Ind. Eng. Chem.* **13**, 1162 (2007).
- [12] T. K. Jayasree and P. Predeep, Effect of fillers on mechanical properties of dynamically crosslinked styrene butadiene rubber/high density polyethylene blends, *J. Elastomers Plast.* **40**, 127 (2008).
- [13] Z. Wang, J. Liu, S. Wu, W. Wang, and L. Zhang, Novel percolation phenomena and mechanism of strengthening elastomers by nanofillers, *Phys. Chem. Chem. Phys.* **12**, 3014 (2010).
- [14] N. A. Bawadukji and R. Jabra, Formulation, preparation, and mechanical characterization of nitrile-butadiene rubber (NBR) composites, *Mater. Sci.: Ind. J.* **15**, 116 (2017).
- [15] J. Plagge, Mastering of filled rubber strength beyond WLF: Competition of temperature, time, crack deflection and bond breaking, *Polymers* **14**, 765 (2022).
- [16] H.-D. Luginsland, *A Review on the Chemistry and the Reinforcement of Silica-Silane Filler System for Rubber Applications* (Shaker Verlag, Aachen, Germany, 2002).
- [17] C. Wrana, *Introduction to Polymer Physics* (LANXESS AG, Leverkusen, Germany, 2009).
- [18] L. Nikiel, W. Wampler, J. Neilsen, and N. Hershberger, How carbon black affects electrical properties, *Rubber & Plast. News* March **23**, 12 (2009).
- [19] T. A. Vilgis, G. Heinrich, and M. Klüppel, *Reinforcement of Polymer Nano-composites* (Cambridge University Press, Cambridge, 2009).
- [20] H. Xi and R. Hentschke, The influence of structure on mechanical properties of filler networks via coarse-

- grained modeling, *Macromol. Theory Simul.* **23**, 373 (2014).
- [21] G. Heinrich, M. Klüppel, and T. A. Vilgis, Reinforcement of elastomers, *Curr. Opin. Solid State Mater. Sci.* **6**, 195 (2002).
- [22] V. N. Khiêm and M. Itskov, Analytical network-averaging of the tube model: Strain-induced crystallization in natural rubber, *J. Mech. Phys. Solids* **116**, 350 (2018).
- [23] F. Bueche, Tensile strength of plastics above the glass temperature, *J. Appl. Phys.* **26**, 1133 (1955).
- [24] J. Meyer, R. Hentschke, J. Hager, N. W. Hojdis, and H. A. Karimi-Varzaneh, Molecular simulation of viscous dissipation due to cyclic deformation of a silica-silica contact in filled rubber, *Macromolecules* **50**, 6679 (2017).
- [25] R. Hentschke, The Payne effect revisited, *Express Polym. Lett.* **11**, 278 (2017).
- [26] R. Hentschke, Macroscopic mechanical properties of elastomer nano-composites via molecular and analytical modelling, *Soft Mater.* **16**, 315 (2018).
- [27] J. Plagge (private communication).
- [28] I. Kende, T. L. Pickering, and A. V. Tobolsky, The dissociation energy of the tetrasulfide linkage, *J. Am. Chem. Soc.* **87**, 5582 (1965).
- [29] V. M. Litvinov, R. A. Orza, M. Klüppel, M. van Duin, and P. C. M. M. Magusin, Rubber filler interactions and network structure in relation to stress strain behavior of vulcanized, carbon black filled EPDM, *Macromolecules* **44**, 4887 (2011).
- [30] A. Schröder, Charakterisierung verschiedener Russtypen durch systematische statische Gasadsorption—Energetische Heterogenität und Fraktalität der Partikeloberfläche, Ph.D thesis, Universität Hannover, Germany (2000).
- [31] R. Hentschke, B. L. Schürmann, and J. P. Rabe, Molecular dynamics simulations of ordered alkane chains physisorbed on graphite, *J. Chem. Phys.* **96**, 6213 (1992).
- [32] W. M. Hess and G. C. McDonald, Improved particle size measurements on pigments for rubber, *Rubber Chem. Technol.* **56**, 892 (1983).
- [33] R. W. Sambrook, Influence of temperature on the tensile strength of carbon filled vulcanizates, *Rubber Chem. Technol.* **44**, 728 (1971).
- [34] S.-Y. Fu, X.-Q. Feng, B. Lauke, and Y.-W. Mai, Effects of particle size, particle/matrix interface adhesion and particle loading on mechanical properties of particulate-polymer composites, *Composites B* **39**, 933 (2008).
- [35] R. Hentschke, *Classical Mechanics* (Springer, Heidelberg, 2017).
- [36] G. Landon, G. Lewis, and G. F. Boden, The influence of particle size on the tensile strength of particulate-filled polymers, *J. Mater. Sci.* **12**, 1605 (1977).
- [37] B. Pukanszky and G. Vörös, Mechanism of interfacial interactions in particulate filled composites, *Compos. Interfaces* **1**, 411 (1993).
- [38] F. Bueche, Tensile strength of filled SBR vulcanizates, *Rubber Chem. Technol.* **32**, 680 (1959).
- [39] T. L. Smith, Dependence of the ultimate properties of a GR-S rubber on strain rate, *J. Polym. Sci.* **32**, 99 (1958).
- [40] A. E. Oberth, Principle of strength reinforcement in filled rubbers, *Rubber Chem. Technol.* **40**, 1337 (1967).
- [41] H. W. Greensmith, Rupture of rubber. VII. Effect of rate of extension in tensile tests, *Rubber Chem. Technol.* **34**, 76 (1961).
- [42] T. J. Dudek and F. Büche, Tensile strength of gum and reinforced EPR and SBR vulcanizates, *Rubber Chem. Technol.* **37**, 818 (1964).
- [43] T. L. Smith, Strength of elastomers. A perspective, *Rubber Chem. Technol.* **51**, 225 (1978).
- [44] Z. Song, T. Shen, F. J. Vernerey, and S. Cai, Force-dependent bond dissociation explains the rate-dependent fracture of vitrimers, *Soft Matter* **17**, 6669 (2021).